DOI: 10.1002/ejic.200901044

Hydrocarbon Oxygenation by Metal Nitrite Adducts: Theoretical Comparison with Ferryl-Based Oxygenation Agents

Radu Silaghi-Dumitrescu*[a] and Sergei V. Makarov[b]

Keywords: Iron / Heme proteins / Oxygenation / Cytochromes / Redox chemistry

Metal nitrite adducts can, under certain conditions, insert one of their oxygen atoms into hydrocarbons. This reaction is to some extent reminiscent of the process whereby high-valent ferryl (formally Fe^{IV}=O) species such as compound I in hemoproteins also insert an oxygen atom into hydrocarbons. Density functional theory (DFT) data are shown here, examining the oxygenation ability of ferrous and ferric nitrite adducts in octahedral coordination environments modeling those seen in hemoproteins where such adducts are well characterized. A comparison of these results with those obtained with similar methods on formal Fe^{V}–oxido models of hemoprotein compound I models relevant for such enzymes as cytochrome P450 and chloroperoxidase reveals a key role of the redox potential in dictating oxygenation ability, in good agreement with interpretations previously given by Green and co-workers.

Introduction

Hydrocarbon activation via oxygen atom insertion and/or hydrogen atom abstraction is achieved selectively and efficiently by high-valent (formally Fe^{V}) centers of which compound I species seen in hemoproteins such as peroxidases and cytochrome P450 have received much interest.[1–18] Compound I species typically involve an Fe^{IV} center bound to an oxido ligand, Fe^{IV}=O (ferryl), with one more reducing equivalent located on the porphyrin ligand as a cation radical.[12,17,18] Among the factors controlling the oxygen-inserting and hydrogen-atom-abstracting reactivity of these ferryl centers, the basicity of the oxido ligand (possibly in connection with the generation of a protonated ferryl as a prerequisite for the reaction), the spin density at the oxygen atom correlated with the high degree of covalence within the Fe^{IV}–oxido bond, the redox potential, and the availability of low-lying excited states have been discussed.[1–18] It is also known that compound II species, which feature ferryl groups without the additional extra oxidizing equivalent on the porphyrin, and also ferric–oxido centers, are less reactive towards hydrocarbons.[19,20] On the other hand, metal nitrite adducts in the nitro isomer are also known to hydroxylate or epoxidize hydrocarbons.[21,22] While their reactivity towards hydrocarbons is distinctly lower than that of ferryl-containing compound I species,[21,22] a comparison between the hydrocarbon-activating properties of the ferryl oxygen with the nitro oxygen in a metal nitrite adduct may be expected to offer insight into the factors controlling hydrocarbon oxidation/oxygenation by metal complexes. Thus, density functional theory (DFT) data are presented here, comparing the oxygen atom donation and hydrogen atom abstraction reactions by models of hemoprotein ferryl-containing compound I and models of iron nitrite adduct with biologically relevant ligands.

Results and Discussion

We have previously described the potential energy surface for hydrogen atom abstraction from a methane molecule by a model of the cytochrome P450 compound I such as that depicted in Figure 1, and for which an energy barrier of ca. 18 kcal/mol was predicted at the level of theory employed in the present study.[23] Figure 1 illustrates the performance of a simple octahedral iron–nitro model, in its ferrous and ferric forms, in performing the same reaction employing this time not a ferryl but rather a nitro oxygen atom. Thus, for the Fe^{II}–nitro case, hydrogen atom abstraction appears entirely unfeasible. Remarkably, however, the energy required for hydrogen atom transfer from methane to one of the two equivalent oxygen atoms in the ferric–nitro model appears to be within the same range as that previously computed for P450 compound I. The key stage of this process, according to Figure 1, appears to be at oxygen–hydrogen distances of 1.3 Å and shorter, where the ferrous and ferric states behave drastically different. Indeed, examination of the spin densities within the ferric–nitro model, illustrated in Figure 2, shows that as the O(nitro)–H(methane) distance is lowered in the ferric model, the spin density migrates from the iron (≈one full unit on iron at equilibrium) to the methane carbon atom. This is consistent with an electron being transferred from the hydrocarbon to the iron, resulting in a radical on the methane and a Fe^{II}

[a] "Babes-Bolyai" University,
Cluj-Napoca 400028, Romania
Fax: +40-264590818
E-mail: rsilaghi@chem.ubbcluj.ro
[b] State University of Chemistry and Technology,
Engels str. 7, 153000 Ivanovo, Russia

center. Notably, at an O(nitro)–H(methane) distance of 1.30 Å, where most of this electron transfer has essentially occurred, the carbon–hydrogen bond length is still slightly shorter than 1.30 Å, at 1.26 Å, implying that proton transfer occurs subsequent to electron transfer. Furthermore, subsequent steps on the reaction coordinate, from 1.30 Å further towards a proper O–H bond, are all done at essentially no further energy cost, implying that most of the rise in energy along the reaction coordinate has come from transfer of electron density, prior to transfer of the proton. Under these conditions, with the first step consisting of an electron transfer, the redox potential of the hydrogen-abstracting species does appear to be a key factor, thus explaining the distinctly better reactivity in the ferric–nitro adduct compared to the ferrous–nitro counterpart. This finding is in line with previous observations by Green and co-workers on the importance of the redox potential in controlling the reactivity of compound I in hemoproteins and related systems, while also downplaying the role of the basicity of the oxygen atom in hydrogen-atom-abstracting reactions:[1] indeed, Figure 1 shows that the oxygen atom in the ferrous–nitro models, despite having more electron density available than the oxygen atom in the ferric–nitro counterpart, performs far worse in abstracting a hydrogen atom from the hydrocarbon. Also notable is the fact that while the oxygen atom in compound I carries ≈one spin unit, making it somewhat akin to a hydroxyl radical and therefore presumably more adept at abstracting hydrogen atoms, there is only negligible spin density on the oxygen atom in the ferric–nitrite model 1 prior to reaction with methane; yet, the energy required for hydrogen atom abstraction by these very different oxygen atoms is very similar, suggesting that pre-existing spin density of the oxygen atom is not a prerequisite for the reaction.

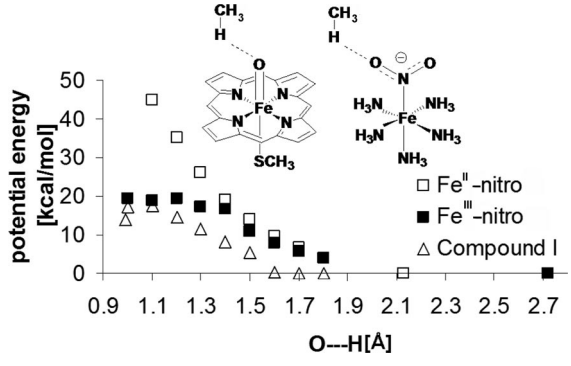

Figure 1. Variation of the potential energy as a function of the O···H distance (in Å) during hydrogen atom abstraction from methane by thiolate ligated compound I or by a ferric or ferrous–nitro adduct (structures shown). Geometries were optimized with the O···H distance (dotted lines in chemical structures shown as inset) constrained to values indicated in the plots (empty squares and triangles, respectively), starting from the 1.8-Å state and decreasing the O···H distance by amounts indicated in the plot. For each model, energy differences are plotted with the energy of the reactants (far right side of the plot) taken as reference.

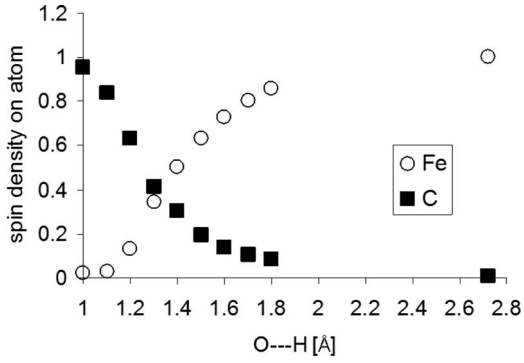

Figure 2. Evolution of spin densities on iron and carbon along the reaction coordinate for the Figure 1 process involving hydrogen atom abstraction from methane by the ferric nitrite model.

A final note on Figure 1 is to be made on the fact that the product of hydrogen atom abstraction by the ferric–nitro adduct does not appear to be a stable local minimum; this is in line with experimental data according to which nitrite adducts do not hydroxylate hydrocarbons under the same mild conditions as hemoprotein compound I species do. This part of the difference in potential energy surfaces between ferric–nitro and compound I models can be now traced to the basicity of the oxygen atom: its protonation by the hydrogen atom arriving from methane would, if it was more energetically favorable, lower the energy of the left-most data points in the Figure 1 potential energy surface and stabilize the end product to the point where the reaction would indeed be feasible.

A second reaction type achieved by compound I systems is epoxidation of carbon–carbon double bonds. In principle, the mechanism of this process may follow two routes, as illustrated in Scheme 1: a concerted route or a sequential one. Figure 3 illustrates the performance computed for the ferrous– and ferric–nitro models versus P450 compound I in the first stage of a sequential epoxidation mechanism; attempts to locate low-energy reaction pathways for a concerted mechanism in the nitro adducts failed and are not discussed.

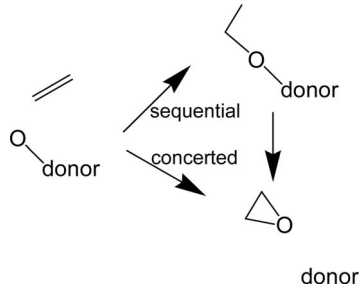

Scheme 1.

Notable in Figure 3 is the behavior of the three systems in the epoxidation reaction, very similar to what was seen for the hydroxylation reaction of Figure 1. Thus, once again the ferric–nitro adduct appears distinctly more reactive than its ferrous counterpart and similar to the compound I model from this point of view. As the O(ferric–nitro)–car-

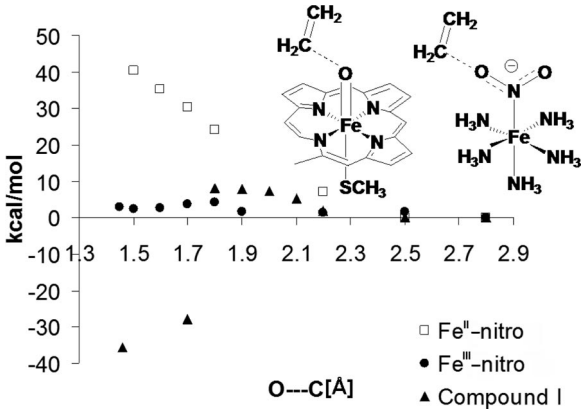

Figure 3. Variation of the potential energy as a function of the O···C distance (in Å, indicated as dotted line in structures shown) during hydrogen atom abstraction from methane by thiolate-ligated compound I or by a ferric– or ferrous–nitro adduct (structures shown). Geometries were optimized with the O···C distance (dotted lines in chemical structures shown as inset) constrained to values indicated in the plots (empty squares and triangles, respectively), starting from the 2.8-Å state and decreasing the O···C distance by amounts indicated in the plot. For each model, energy differences are plotted with the energy of the reactants (far right side of the plot) taken as reference.

bon(ethylene) distance is shortened, a gradual transfer of spin density is seen to occur from the iron to the second carbon atom in ethylene (cf. Figure 4). Importantly, while the ferric–nitro potential energy surface reaches a maximum in Figure 3 at ca. 1.9 Å, well before a proper carbon–oxygen bond has been established, Figure 4 shows that at this point (1.9–2.0 Å on the reaction coordinate) much of the electron transfer form iron to the hydrocarbon has already occurred. Thus, once again the process is primarily redox in nature, which among other things explains why the ferrous–nitro species is computed to be much less reactive.

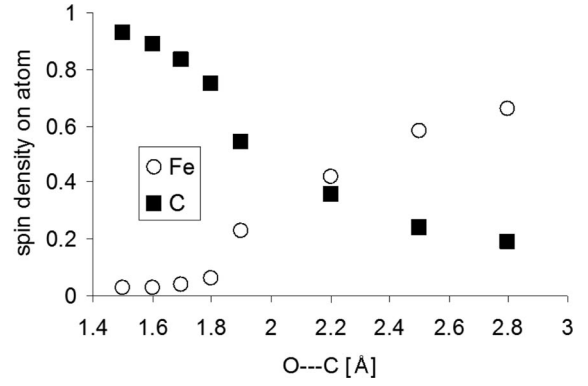

Figure 4. Evolution of spin densities on iron and carbon along the reaction coordinate for the Figure 3 process involving oxygen atom transfer the ferric–nitrite model to a carbon atom in ethylene.

Conclusions

In conclusion, comparison of the ferryl-type and ferric/ferrous–nitro oxygenating reagents allows two main factors to be identified in controlling hydrocarbon activation via the oxygen atoms in these centers. First of all, the redox potential of the metal complex appears to be the main factor as electron transfer appears to be complete prior to completion of bond breaking and formation. The second factor, indirectly correlated in fact to the redox potential, is the basicity of the oxygen atom. Although the hydrogen atom abstraction reactions by definition entail free radicals and may hence be assumed to benefit from the oxygen atom carrying large amounts of spin density in the ferryl group, the amount of spin density localized on the oxygen atom in the "resting state" (prior to reaction) and the precise type of electronic structure (diradical with dioxygen-type structure in ferryl, or plain closed-shell nitrite ligand) has negligible importance relative to the redox potential and basicity.

Experimental Section

Figure 1 shows the models examined in the present study. For compound I, an unsubstituted heme, methanethiolate, and an oxido atom were used as ligands to the iron, and the overall charge was set to 0, accounting for a formally Fe^{V} center as described previously, with a net spin state of $S = 1/2$.[23] For the nitro models, the ligands were five ammonia molecules and a nitrite anion; low-spin states were assumed and the overall charge was set to +1 and +2 respectively, accounting for a formally Fe^{II} or formally Fe^{III} center as indicated in the figures. Geometries were optimized at the DFT level in the Spartan software package[24] without any constraints other than those specified in the figures along the reaction coordinates. Potential energy surfaces were explored by variation of the distance between the oxygen atom of the ferryl group in compound I models or from the nitro group of the nitro models, and the hydrogen atom in the hydrocarbon (for hydrogen atom abstraction reactions; methane chosen as model hydrocarbon) or one of the carbon atoms of an ethylene molecule (for the epoxidation reactions). Initial oxygen–hydrogen distances for hydrogen-abstraction reactions were set to 1.8 Å for reasons previously detailed in ref.;[23] for the same reasons (relevance for the geometry adopted in cytochrome P450 enzyme active sites, where substrates are placed in such close proximity to the iron[23]), the initial carbon–oxygen atom for the epoxidation reactions were set to 2.8 Å. This protocol is expected to give a reasonable estimate of the barrier heights; a proper transition search would give even more accurate values. The BP86 functional, which uses the gradient corrected exchange functional proposed by Becke (1988)[25] and the correlation functional by Perdew (1986),[26] and the 6-31G** basis set were used as implemented in Spartan. For the SCF calculations, a fine grid was used and the convergence criteria were set to 10^{-6} (for the root-mean square of electron density) and 10^{-8} (energy), respectively. For geometry optimization, convergence criteria were set to 0.001 au (maximum gradient criterion) and 0.0003 (maximum displacement criterion). This approach has previously yielded satisfactory results on similar complexes.[14,23,27–30] Charges and spin densities were derived from NBO population analyses after DFT geometry optimization.

Acknowledgments

Funding from a joint Russian Foundation for Basic Research/Romanian Academy (to S. V. M. and R. S. D.), as well as from the Romanian Government (Ideas project 565/2007 to R. S. D.) is gratefully acknowledged.

[1] M. T. Green, J. H. Dawson, H. B. Gray, *Science* **2004**, *304*, 1653–1656.
[2] M. T. Green, *J. Am. Chem. Soc.* **2006**, *128*, 1902–1906.
[3] R. K. Behan, M. T. Green, *J. Inorg. Biochem.* **2006**, *100*, 448–459.
[4] R. K. Behan, L. M. Hoffart, K. L. Stone, C. Krebs, M. T. Green, *J. Am. Chem. Soc.* **2006**, *128*, 11471–11474.
[5] K. L. Stone, R. K. Behan, M. T. Green, *Proc. Natl. Acad. Sci. USA* **2005**, *102*, 16563–16565.
[6] K. L. Stone, L. M. Hoffart, R. K. Behan, C. Krebs, M. T. Green, *J. Am. Chem. Soc.* **2006**, *128*, 6147–6153.
[7] K. L. Stone, R. K. Behan, M. T. Green, *Proc. Natl. Acad. Sci. USA* **2006**, *103*, 12307–12310.
[8] B. Meunier, S. P. de Visser, S. Shaik, *Chem. Rev.* **2004**, *104*, 3947–3980.
[9] S. Shaik, S. P. de Visser, F. Ogliaro, H. Schwarz, I. Schröder, *Curr. Opin. Chem. Biol.* **2002**, *6*, 556–567.
[10] S. Shaik, S. Cohen, S. P. de Visser, P. K. Sharma, D. Kumar, S. Kozuch, F. Ogliaro, D. Danovich, *Eur. J. Inorg. Chem.* **2004**, 207–226.
[11] S. Shaik, S. P. de Visser, D. Kumar, *J. Am. Chem. Soc.* **2004**, *126*, 11746–11749.
[12] S. Shaik, S. P. de Visser, D. Kumar, *J. Biol. Inorg. Chem.* **2004**, *9*, 661–668.
[13] S. Shaik, D. Kumar, S. P. de Visser, A. Altun, W. Thiel, *Chem. Rev.* **2005**, *105*, 2279–2328.
[14] R. Silaghi-Dumitrescu, *J. Biol. Inorg. Chem.* **2004**, *9*, 471–476.
[15] R. Silaghi-Dumitrescu, *Rev. Chim.* **2007**, *58*, 461–464.
[16] R. Silaghi-Dumitrescu, B. J. Reeder, P. Nicholls, C. E. Cooper, M. T. Wilson, *Biochem. J.* **2007**, *403*, 391–395.
[17] M. Sono, M. P. Roach, E. D. Coulter, J. H. Dawson, *Chem. Rev.* **1996**, *96*, 2841–2888.
[18] D. L. Harris, *Curr. Opin. Chem. Biol.* **2001**, *5*, 724–735.
[19] C. E. MacBeth, R. Gupta, K. R. Mitchell-Koch, V. G. Young Jr., G. H. Lushington, W. H. Thompson, M. P. Hendrich, A. S. Borovik, *J. Am. Chem. Soc.* **2004**, *126*, 2556–2567.
[20] C. E. MacBeth, A. P. Golombek, V. G. Young Jr., C. Yang, K. Kuczera, M. P. Hendrich, A. S. Borovik, *Science* **2000**, *289*, 938–941.
[21] S. K. O'Shea, W. Wang, R. S. Wade, C. E. Castro, *J. Org. Chem.* **1996**, *61*, 6388–6395.
[22] C. E. Castro, S. K. O'Shea, *J. Org. Chem.* **1995**, *60*, 1922–1923.
[23] R. Silaghi-Dumitrescu, C. E. Cooper, *Dalton Trans.* **2005**, 3477–3482.
[24] *Spartan 5.0*, Wavefunction, Inc., 18401 Von Karman Avenue Suite 370, Irvine, CA, U.S.A..
[25] A. D. Becke, *Phys. Rev.* **1988**, 3098–3100.
[26] J. P. Perdew, *Phys. Rev. B* **1986**, *33*, 8822–8824.
[27] R. Silaghi-Dumitrescu, *Inorg. Chem.* **2004**, *43*, 3715–3718.
[28] R. Silaghi-Dumitrescu, *J. Inorg. Biochem.* **2006**, *100*, 396–402.
[29] R. Silaghi-Dumitrescu, I. Silaghi-Dumitrescu, *J. Inorg. Biochem.* **2006**, *100*, 161–166.
[30] R. Silaghi-Dumitrescu, *Eur. J. Inorg. Chem.* **2008**, 5404–5407.

Received: December 2, 2009
Published Online: January 19, 2010

